UCRL-JC-151998

LAWRENCE
LIVERMORE
NATIONAL
LABORATORY

Hohlraum-Driven Ignition-Like Double-Shell Implosion Experiments on Omega: Analysis and Interpretation

P. Amendt, H.F. Robey, H.-S. Park, R.E. Turner, R.E. Tipton, J.L. Milovich, J.D. Colvin, M.J. Edwards, R. Hibbard, H. Louis, R. Wallace, D.P. Rowley, W.S. Varnum, R.G. Watt, D.C. Wilson, W. Garbett, A.M. Dunne

August 22, 2003

3rd IFSA Conference, Monterey, CA, September 7-12, 2003

This work was performed under the auspices of the U.S. Department of Energy by University of California, Lawrence Livermore National Laboratory under Contract W-7405-Eng-48.

TuO4.4

HOHLRAUM-DRIVEN IGNITION-LIKE DOUBLE-SHELL IMPLOSION EXPERIMENTS ON OMEGA: ANALYSIS & INTERPRETATION

Peter Amendt, H.F. Robey, H.-S. Park, R.E. Turner, R.E. Tipton, J.L. Milovich, J.D. Colvin, M.J. Edwards, R. Hibbard, H. Louis, R. Wallace, D.P. Rowley
Lawrence Livermore National Laboratory, Livermore, CA USA 94550

W.S. Varnum
Comforce Technical Services. Inc. at LANL, Los Alamos, NM 87545

R.G. Watt, D.C. Wilson
Los Alamos National Laboratory, Los Alamos, NM USA 87545

W. Garbett and A.M. Dunne
AWE Aldermaston, UK

ABSTRACT. *An experimental campaign to study hohlraum-driven ignition-like double-shell target performance using the Omega laser facility is in has begun. These targets are intended to incorporate as many ignition-like properties of the proposed National Ignition Facility (NIF) double-shell ignition design [1,2] as possible, given the energy constraints of the Omega laser. In particular, this latest generation of Omega double-shells is nominally predicted to produce over 99% of the (clean) DD neutron yield from the compressional or stagnation phase of the implosion as required in the NIF ignition design. By contrast, previous double-shell experience on Omega [3] was restricted to cases where a significant fraction of the observed neutron yield was produced during the earlier shock convergence phase where the effects of mix are deemed negligibly small. These new targets are specifically designed to have optimized fall-line behavior for mitigating the effects of pusher-fuel mix after deceleration onset and, thereby, providing maximum neutron yield from the stagnation phase. Experimental results from this recent Omega ignition-like double-shell implosion campaign show favorable agreement with two-dimensional integrated hohlraum simulation studies when enhanced (gold) hohlraum M-band (2-5 keV) radiation is included at a level consistent with observations.*

I. INTRODUCTION

Interest in demonstrating double-shell ignition on the NIF is growing owing to the expected ease in target preparation and fielding at room temperature. Compared with the baseline cryogenic ignition design [4], the ignition double-shell target design is complementary in the following respects: (1) the requested laser power history is less demanding, leaving less stringent requirements on shock sequencing; (2) the reverse-ramp nature of the laser power shape leaves little time for the hohlraum to fill with plasma, possibly providing less laser backscatter from problematic laser-plasma interactions (LPI); (3) hohlraum (thermal) flux symmetry requirements are milder owing to the relatively low convergences of the outer shell ($\approx$3) and inner shell ($\approx$10); (4) threshold ignition temperatures and peak implosion velocities are nearly a factor-of-two lower; (5) the mid- to high-Z inner-shell composition makes the double-shell more vulnerable to deleterious atomic mix compared with the cryogenic DT design; (6) the mode of ignition is volume rather than hot-spot; and (7) the thermonuclear yield of a double-shell is nearly 10$\times$ lower than the baseline design despite a high burn fraction. Achieving double-shell ignition on the NIF will involve its own set of demanding fabrication requirements, from the construction of smooth (seamless) high-Z shells with high-pressure DT fill to the assembly of highly concentric inner- and outer-shells. The main design challenge is controlling atomic mix to levels that will not thwart ignition and assuring that hard x-ray flux asymmetry from laser spots will not seriously degrade implosion symmetry. If too much high-Z pusher material migrates to target center, the local cooling effects will preempt ignition. By virtue of the high-Z nature of the inner shell, hard x rays from the laser-heated hohlraum wall material are efficiently absorbed and may adversely affect implosion symmetry. Control of these problematic effects is necessary before the prospects for double-shell ignition can markedly improve.

A useful figure-of-merit for gauging the robustness of an imploding target to fuel-pusher mix is the fall-line of the inner surface of the inner-shell. The fall-line is the straight-line trajectory of radially converging material following the instant of deceleration onset. By causality, little if any pusher material should reside ahead of the fall-line. Thus, a delayed fall-line trajectory relative to thermonuclear burn should provide added robustness to fuel-pusher mix. A design goal is to optimize fall-line behavior in order to minimize the effects of instability-induced atomic mix of fuel and pusher material. This point-of-view has been applied to a previously described NIF double-shell target design [2].

To make some headway in overcoming the above challenges faced in achieving double-shell ignition on the NIF, preliminary experiments are underway on the Omega laser facility [5]. Although the energy available on the Omega laser is well below the threshold for achieving ignition, useful scaled experiments can be conducted to test our understanding of double-shell implosion performance. Our aim in this work is to emulate as many properties of an igniting double-shell as possible. Some accessible properties include the peak implosion speed ($\approx$220 μm/ns), high target convergence (outer shell radius over imploded fuel radius >30), a nearly constant x-ray drive history, and fall-line optimization. A particular focus of this experimental campaign is demonstrating significant neutron yield from the compressional stage of the implosion compared with the earlier shock flash phase. The compressional stage of neutron burn provides a good test of mix control since the earlier shock-flash stage occurs before any significant development of hydrodynamic instability growth. A convenient and traditional metric of implosion performance is the ratio of the measured neutron yield over the simulated clean neutron yield, i.e., "YoC". A high YoC value does not necessarily imply successful control of mix since some (clean) neutron burn histories may be dominated by the shock flash stage. This scenario can occur when the pusher has been significantly x-ray preheated, leading to enhanced burn from the converging dominant shock at the expense of compressional yield. Often the YoC for such an implosion is respectably high, masking the fact that the overall clean neutron yield has been significantly suppressed. Clearly, such an "exploding pusher" mode is not ignition-like in the sense that significant compressional yield (>99%) is not observed. The previous (cylindrical) hohlraum-driven double-shell database [3] on Nova and Omega can be grouped into two categories: (1) implosions with high YoCs (50-100%) but relatively low (clean) compressional yields, and (2) rather low YoC (<2%) ignition-like implosions. A vexing challenge for double-shell research is explaining the legacy of underperforming targets while demonstrating suitable control of mix as a prerequisite for achieving ignition-like behavior, i.e., high compressional neutron burn fractions (>99%).

We present results from a recent Omega double-shell implosion campaign that set out to demonstrate ignition-like behavior. Three main objectives were met: (1) demonstrating significant compressional neutron burn fraction (20-35%), (2) obtaining a reproducible, high-quality dataset, and (3) achieving core x-ray images of an imploded double-shell.

II. EXPERIMENT AND RESULTS

Four types of implosion targets were fielded on the Omega laser facility. The first class of target was single-shell surrogate capsules, intended to mimic the hohlraum radiation environment of a double-shell target and to calibrate and align the x-ray and neutron diagnostics [See Fig. 1(a)]. These targets were followed by two "M-band" imaging double-shell targets that were designed to measure Au M-shell (2-5 keV) x-ray strength at the center of the scale-1 gold hohlraum [See Fig. 1(b)]. The basic principle of the M-band target is to radiograph the implosion trajectory of a glass micro-balloon that is principally driven by M-band x rays. The role of the oversized outer shell is to shield the inner shell from

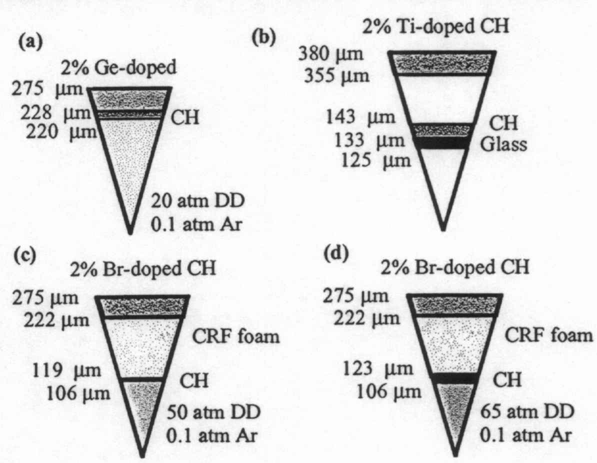

Fig. 1(a-d): Nominal dimensions for (a) single-shell surrogate capsule, (b) M-band imaging target, (c) thin shell inner-shell double-shell and (d) thick inner-shell double-shell.

thermal x rays (< 1 keV) and to delay shell collision, leaving the inner shell free to implode under the action of M-band absorption. The plastic overocoating on the inner microballoon helps tamp the radial expansion of the M-band heated glass and promotes inward convergence. A chromium backlighter is used for radiographing the imploding glass shell at 5.6 keV; multiple x-ray images of the imploding shell were obtained using an array of 10 μm pinholes and 70 ps resolution framing cameras.

Following these preparatory targets, several double-shell implosion targets were then fielded. Figure 1(c) shows the "thin-shell" version with Ar dopant of the DD fuel for facilitating core self-emission (4-6 keV), while Fig. 1(d) shows a thicker inner-shell version but absent the dopant. The machined carbonized-resorcinal-formaldehyde (CRF) foam hemispherical inserts were used to support the inner shell and to ensure shell concentricity to within 5 μm. This foam material was chosen because of its machining properties and inherently small pore size (<100 nm). A relatively small pore size provides more margin to seeding of destructive hydrodynamic instability growth. The outer shell consisted of two hemispherical shells with a machined step joint that were spot-joined with a low-Z epoxy. Both types of double-shell target were designed for optimum fall-line behavior and high compressional neutron yield fraction (>99%). A dimensionless fall-line parameter is defined as the difference between the instant of peak neutron burn and the fall-line reaching the origin, normalized to the FWHM of the neutron burn history. The requested laser power history was a reverse ramp

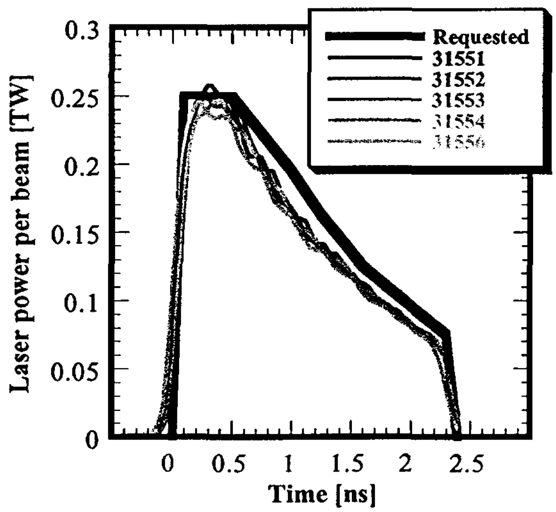

Fig. 2: Requested and delivered laser power profiles for several double-shell implosions.

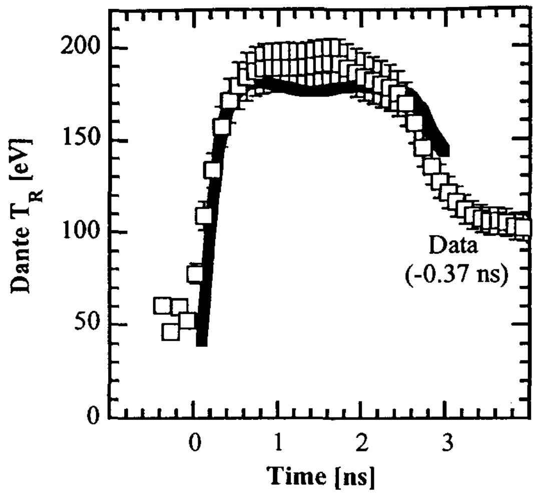

Fig. 3: Measured and simulated Dante drive temperature comparison for type-1 double-shell target [Fig. 1(c)].

[See Fig. 2], designed to deliver a nearly constant hohlraum drive temperature of nearly 185 eV over 2 ns. Three cones consisting of 5, 5, and 10 laser beams enter each end of the cylindrical gold hohlraum through a laser-entrance hole (LEH) at three distinct angles to the hohlraum symmetry axis: θ=21.4°, 42°, and 58.9°. The hohlraums were 2500 μm long, with a diameter of 1600 μm and 75% LEHs. Overall, the delivered energy was about 10% lower than requested, giving less than optimal fall-line behavior for each target. The radiation drive temperature was monitored with an array of calibrated x-ray diodes (Dante [6]) looking through the LEH at 37° to the symmetry axis. Figure 3 shows that the comparison between measured and post-processed 2-D radiation-hydrodynamics simulations is well within the measurement uncertainties. Full-aperture backscatter measurements on the outer two cones (42°, 58.9°) show total backscatter levels of less than 200 J. This low backscatter level is expected because of the benign nature of the laser pulse-shape: peak power occurs well before the hohlraum has filled with Au plasma. Measured peak x-ray and neutron emission times [7] from the imploded core provide a further check on the hohlraum drive. Figure 4 shows the measured emission times versus calculated x-ray peak emission times for three surrogate single-shell targets [See Fig. 1(a)] and for a type-1 double-shell implosion target. The measured x-ray peak emission times appear to be systematically early by ≈200 ps, which is within the absolute timing uncertainty.

An important feature of an indirectly-driven double-shell implosion is the degree of x-ray preheat incident on the inner-shell. Two independent M-band diagnostics are

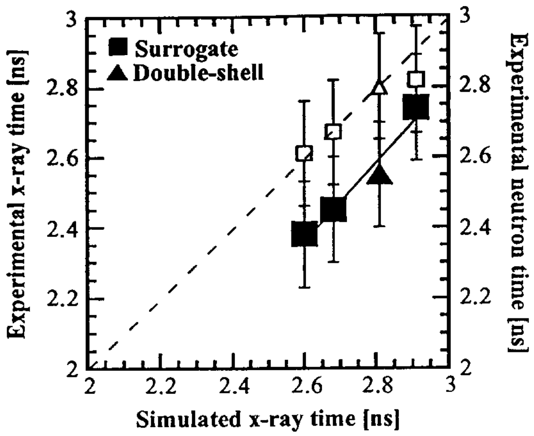

Fig. 4: Measured x-ray (solid) and neutron (open) peak emission times versus simulated x-ray peak emission times for three single-shell surrogates (squares) and type-1 double-shell target (triangle).

available for inferring the amount of M-band preheat. First, the highest energy channel of Dante provides a time-dependent record of 2-5 keV radiation exiting the LEH. In addition, the M-band imaging double-shell provides an integrated test of preheat strength at target center. Figure 5 shows the measured and simulated M-band x-ray fraction versus time according to Dante. The nominal non-LTE calculation with shell-averaged Au opacities (XSN) underestimates the data by more than a factor-of-two up to 1.5 ns and agrees with the data only after 2 ns. To effect a better match with the data, time-dependent Au emissivity opacities above 2 keV were applied in the simulations as shown in Fig. 5. This empirical procedure had little effect on the overall thermal x-ray drive history [Fig. 3], giving at most a 2-3 eV increase in the drive temperature. An independent check of the simulated M-band deficit can be obtained by studying the M-band double-shell imaging data [See Fig. 1(b)]. By analyzing the trajectory of the imploding glass microballoon with and without the Au emission opacity multipliers, further support for enhanced M-band in the experiment can be found. Figure 6 shows such a comparison, clearly indicating that the data is more consistent with M-band enhancement than without. The 200 ps shift in the data is consistent with Fig. 4 which also shows a similar temporal offset in the observed peak x-ray emission times.

Constraining the x-ray drive is crucial for lending credibility to a simulated neutron yield (or YoC). Figures 3-6 collectively establish a fairly consistent picture of the level of thermal and M-band x-ray drive in the experiment. Our considerable focus on M-band is derived from the expected sensitivity of an Omega-scale double-shell implosion to preheat. With the limited energy available on Omega for the prescribed pulse-shape [See Fig. 3], the inner-shell must be thin enough to reach a sufficiently high implosion velocity - but not so thin that feed-thru of hydrodynamic instability from the outside surface to the inner surface can lead to shell breakup. For such thin inner-shells, the mean-free-path of an M-band photon is on the order of the shell thickness, leading to unwanted volumetric expansion and reduced hydrodyamical efficiency. Figure 8 summarizes

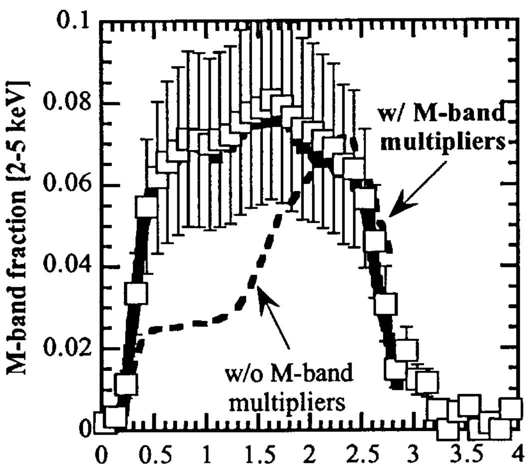

Fig. 5: Measured and simulated Dante M-band fraction versus time for type-1 double-shell with nominal (dashed) and enhanced (solid) Au emission opacity multipliers.

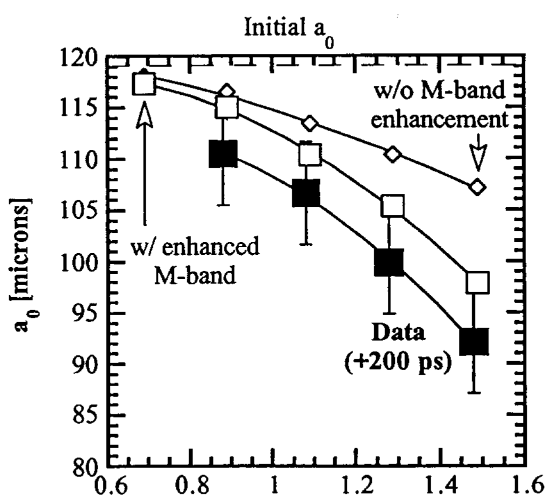

Fig. 6: Measured and simulated trajectory a_0 of 5.6 keV transmission (Cr He-α) minimum with (open squares) and without (open diamonds) Au emission opacity multipliers for M-band imaging double-shell target.

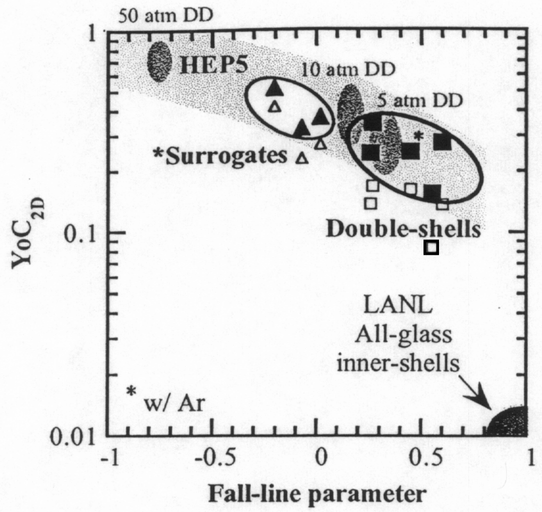

Fig. 8: Observed-over-predicted DD neutron yield versus dimensionless fall-line parameter. Former (HEP5) all-CH single-shell data are shown in dark grey for indicated DD gas-fills. Triangles denote surrogate capsules with (solid) and without (open) enhanced M-band radiation; squares represent the double-shell targets.

the performance of the surrogates and double-shell targets compared with the previous database. The "HEP5" data refer to all-CH single-shell high performance implosions on the Omega laser for various gasfill pressures [8]. The open symbols refer to the behavior with nominal M-band strength; closed symbols include enhanced M-band. As expected, the double-shell targets are more sensitive to M-band preheat than their single-shell counterparts. We see that with the enhanced M-band component, both surrogates and double-shells follow an evident trend of slow decline in performance with increasing fall-line parameter. The performance metric used is YoC_{2D}, meaning that the simulated DD yields take into account calculable two-dimensional intrinisic hohlraum flux asymmetries. The main result of this paper is that the calculated clean behavior of our recent double-shell implosions is a significant fraction of the observed yield, achieving a YoC_{2D} as high as 35%. Furthermore, the performance trend is consistent with the fall-line figure-of-merit metric, thereby further validating its use in ongoing NIF double-shell ignition design efforts. We also argue for the strong role of M-band preheat in double-shells, showing how performance is adversely affected. In particular, calculations show that with enhanced M-band preheat the DD neutron yield drops by more than a factor-of-two, but the (clean) compressional yield fraction still remains above 99%.

We obtained argon self-emission images of the imploded core for the surrogates capsules and the type-1

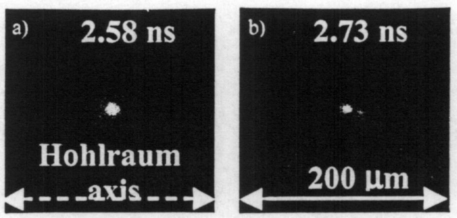

Fig. 9: Self-emission core image of surrogate capsule (a) and type-1 double-shell target (b) with diagnostic timing advanced by 200 ps.

double-shell. Figure 9 shows a nearly round imploded surrogate core, while the double-shell shows some hint of core-splitting. Work is underway to understand this difference and to optimize the photon statistics.

3. SUMMARY

Three main objectives of this Omega double-shell implosion campaign were met: (1) demonstrating significant compressional neutron burn fraction (up to 35%), (2) obtaining a reproducible, high-quality dataset, and (3) achieving core x-ray images of an imploded double-shell. Future work will concentrate on reducing the sensitivity to M-band preheat with a more effective dopant in the outer-shell and understanding lowest-order mode asymmetry of the imploded double-shell core.

4. ACKNOWLEDGMENTS

This work was performed under the auspices of U.S. Department of Energy by the Lawrence Livermore National Laboratory under Contract No. W-7405-Eng-48.

REFERENCES

[1] G.B. HARRIS and W.S. VARNUM, *Bull. Am. Phys.* Soc. **41**, 1479 (1996).

[2] P. AMENDT, J.D. COLVIN, R.E. TIPTON *et al.*, *Phys. Plasmas* **9**, 2221 (2002).

[3] W.S. VARNUM, N.D. DELAMATER, S.C. EVANS *et al.*, *Phys. Rev. Lett.* **81**, 5153 (2000).

[4] S.W. HAAN, S.M. POLLAINE, J.D. LINDL *et al.*, *Phys. Plasmas* **2**, 2480 (1995).

[5] T.R. BOEHLY, D.R. BROWN, R.S. CRAXTON *et al.*, *Opt. Commun.* **133**, 495 (1997).

[6] H.N. KORNBLUM, R.L. KAUFFMAN, and J.A. SMITH, *Rev. Sci. Instrum.* **57**, 2179 (1986)

[7] C. STOECKL, V. YU. GLEBOV, J.D. ZUEGEL, and D.D. MEYERHOFER, *Rev. Sci. Instru.* **73**, 3796 (2002).

[8] P. AMENDT, R.E. TURNER and O.L. LANDEN, *Phys. Rev. Lett.* **89**(16), 165001 (2002).